ICANS-XIV
14th Meeting of the International Collaboration on Advanced Neutron Sources
Starved Rock Lodge, Utica Ill., USA
June 14-19, 1998

Measurements of Heat Transfer at the Beam Window in a Mockup Target for SINQ Using Mercury

I. Platnieks[a], G.S. Bauer[b], O. Lielausis[a] and Y. Takeda[b]

[a]Institute of Physics of the University of Latvia,
[b]Paul Scherrer Institut, Ch-5232 Villigen-PSI, Switzerland

Abstract

Efficient window cooling will be crucial, if a liquid metal target is to be used in the 1 MW spallation source SINQ at some stage, and may have a profound effect on the design of the whole target system. In order to study the wall-to-liquid heat transfer, a Heat Emitting Temperature Sensing Surface (HETSS) was developed and used to measure the temperature difference between the fluid and the wall under different geometric and flow conditions. Turbulence generated by the expanding flow path at the end of the guide tube was found to be efficient even in a geometrically symmetric situation, while thermal convection only plays a role at very small flow rates. Cutting the bottom edge of the guide tube at an angle did not result in any noticeable improvement. Although the results suggest that a hemispherical beam window might be properly cooled without special measures, more controllable configurations will be examined, too.

1. Introduction

One of the main problems in liquid metal target development for high power spallation neutron sources is cooling the beam entrance window. The temperature will, in general, be too high for direct water cooling; at the very minimum it will require a high pressure water system which not only is a source of additional stress on the walls, but also carries the risk of water ingress into the liquid metal in case a leak develops. It would, therefore be highly desirable to be able to cool the window directly by the liquid metal. In order to evaluate this option, knowledge of the flow structure and of the wall-to-fluid heat transfer coefficient is necessary. Although Computational Fluid Dynamics methods have made great progress in recent years in predicting the situation even in complicated geometries, it is still indispensable to perform certain code validation experiments. For this reason a full scale mockup experiment for the SINQ liquid metal target was installed at the large Mercury loop operated by the Institute of Physics of the Latvian University at Riga. In the present paper we report on measurements that aim at determining the heat transfer in the hemispherical cap of the target under different flow conditions which were examined in parallel by an ultrasonic flow mapping technique [1].

Keywords: Liquid metal target; heat transfer, turbulence, Mercury

2. The SINQ target test stand

A schematic drawing of the SINQ target mockup installed at the Mercury loop in Riga is shown in Fig. 1. The lower half of the SINQ target with a diameter of 20 cm and a height of 1500 cm is reproduced in full, while the upper half, which has a diameter of 40 cm and will contain the heat exchanger etc. is only built with reduced height and is meant essentially to serve as a flow distribution and rectification system. The lower part of the inner guide tube and the hemispherical cap can be exchanged to vary the geometry in the cap region and to perform different kinds of measurements. The Mercury flow rate can be varied up to 3.8 l/sec, which is more than what is considered necessary for removing 1 MW of beam power from the SINQ target. Although the operating temperature of the Mercury loop is lower than that of a PbBi target would be, using Mercury for the tests is considered a good choice because it is technically easier than PbBi and all heavy liquid metals are rather similar in their properties. For the present experiments a specially built cap was used which, on its inside, was equipped with a system of Heat Emitting Temperature Sensing Surfaces (HETSS)

3. The Heat Emitting Temperature Sensing Surface

HETSS is a boundary surface between the solid wall and the liquid which is constructed in a way to allow to generate a well defined heat flux density in a selected area and to record the resulting temperature distribution. Technically this is accomplished by forming the surface as an electrically heated resistor for which it is possible to measure the electrical resistance as well as the power dissipation with spatial resolution. By measuring the voltage drop U and the current I in each HETSS element, the dissipated power can be determined from the product U*I of the two quantities, while their ratio U/I gives the resistance, which is temperature dependent. This makes it possible to record the local temperature average over the area of the HETSS. The surface-resistor must be thin enough to have large heat resistance along their length and must be backed by material with poor heat conductivity in order to direct all the heat into the liquid perpendicularly to wall, i.e. with minimum lateral dissipation.

Depending on whether and in what way U and/or I are controlled, the HETSS can be operated in different modes. Ideally, keeping U*I constant would result in a fixed heat flux density and would allow to determine the heat transfer directly as a function of heat flux density. Alternatively, U/I could be kept constant which would mean constant surface temperature and would allow to determine the heat transfer as a function of temperature. In practice it is, of course, easiest to work with a constant current source, which means that the heat flux will depend on the temperature.

Practically the HETSS is produced as a continuous structure of thin copper strips made by the etching technique. Leads for picking up the voltage drop are arranged at suitable positions, while a controlled current is supplied to a larger area for reasons of practicality. In our case (Fig. 2) an area of 21x4 cm^2 was subdivided into three groups with seven units of 4x1 cm^2 each and a separate current source was used to feed each group. This results in

a measuring mode somewhat in between the two limiting cases given above, because only the current rather than the power is controlled.

As an example, Fig 3 gives the measured resistance in the 21 sectors with and without heat flux and the temperature distribution deduced from the measured change in resistance. From top to bottom Fig 3 shows:
- the resistance per surface unit without heat generation
- the resistance measured with the heat flux distribution shown in the frame below
- the heat flux averaged over the respective surface unit
- the temperature distribution deduced from the measured change in resistance.

It is obvious that very precise resistance measurements are required, but several tests have shown that the method gives trustworthy results.

The quantity to be determined for each HETSS unit is the temperature rise per unit heat flux, h (in K/(W/cm^2)), which is the inverse of the heat transfer coefficient:

$$h = \Delta T_s / q \tag{1}$$

The temperature increase on the surface is calculated as

$$\Delta T_s = k_{af} (\Delta T_{Cu} - q \cdot d_i / \lambda_i), \tag{2}$$

where ΔT_{Cu} is the temperature of the copper foil forming the HETSS, k_{af} is the area factor of copper in the HETSS layout (0.8 in the present case) , d_i is the thickness of insulation between the copper and the mercury (75 μm), λ_i is the heat conductance of the insulation (0.39 W\mK for glass textolite as used).

The heat flux density is calculated as

$$q = Q / S, \tag{3}$$

where Q denotes the electrical power supplied to the HETSS element (≈28 W in the present experiment), S is the area of the HETSS element (4 cm^2).

The copper temperature increase is then obtained as

$$\Delta T_{Cu} = (R - r) / r \cdot \alpha, \tag{4}$$

where R is the electrical resistance of the heated HETSS element at full power, r is the electrical resistance of the same element at the temperature of the incoming fluid , α is the temperature coefficient of resistance for copper (0.0044 1/°K).

Both the values of R and r for each HETSS element n were calculated as the ratio of potential drop to the current in the corresponding section at the respective power loads. This current was obtained by means of measuring the potential difference on an instrumental shunt included in the current path. The shunt coefficient equals $k_m = 0.0075$ V/ A.

$$R_n = (U_n / U_m) \cdot k_m \text{ and } r_n = (u_n / u_m) \cdot k_m \tag{5}$$

with n = 1....21, m = 1....3.

The electrical resistance r of HETSS element at the temperature of the incoming flow was obtained at the beginning of the experiment by applying an electrical power which causes a negligible temperature increase (0.0015 W/ cm^2). The changes in the incoming flow temperature are taken into account by means of a continuos measurement of the voltage drop on a special copper resistor. This resistor was connected to a stabilized current source and fixed on the outer pipe of the Mockup where the incoming flow temperature can be determined. The ratio of the actual voltage drop on the resistor to that measured at the beginning of the experiment φ_r / φ_{r0} was used in the computer evaluations as a correction coefficient. (The temperature of the incoming flow was in range 18 ± 1 C° during the experiments.)

The heat flux from a single HETSS element is

$$Q_n = U_n \cdot U_m / k_m \tag{6}$$

The final formula for computer calculations is then

$$h_n = k_{af}\left(\frac{\frac{U_n}{U_m} - \frac{u_n \cdot \varphi_r}{u_m \cdot \varphi_{r0}}}{\alpha \frac{u_n \cdot \varphi_r}{u_m \cdot \varphi_{r0}}} - \frac{U_n \cdot U_m \cdot d_i}{S[m^2] \cdot k_m \cdot \lambda_i}\right) / \frac{U_n \cdot U_m}{S[cm^2] \cdot k_m} . \tag{7}$$

Inserting the fixed quantities for the present experiment, we have

$$h_n = 0.8\left(\frac{\frac{U_n}{U_m} - \frac{u_n \cdot \varphi_r}{u_m \cdot \varphi_{r0}}}{0.0044 \frac{u_n \cdot \varphi_r}{u_m \cdot \varphi_{r0}}} - 64.1 \cdot U_n \cdot U_m\right) / 33.3 \cdot U_n \cdot U_m \tag{7a}$$

For the experiments we are reporting on here, the 21 HETSS elements of 4x1 cm^2 surface area each were arranged in the form of a 4 x 21 cm^2 ribbon imbedded in the hemispherical surface of the bottom cap of the SINQ target mockup. Fig. 4 shows the general arrangement. The bottom cap was produced by arranging the HETSS on a hemispherical dome and casting epoxy on their back side for thermal insulation. After removing the mold the epoxy block was placed into a steel pot with a flange that could be mounted to the bottom end of the outer target tube in different angular positions. The outer surface of the HETSS was covered with a thin layer (0.75 μm of glass textolite) for electrical insulation from the Mercury. As shown in Fig. 4, the labeling of these positions was with respect to the Mercury loop, with 0° being in the loop plane and counting clockwise when viewed from the top. Fig. 4 also shows how the HETSS were numbered from 1 to 21.

The electrical connections and the link with the computerized data acquisition system (cf. Fig. 2) are build to have suitable signal levels for the electronics and to avoid high voltages on the HETSS insulation. The simplification of electrical circuit by going from separately controllable power supplies for each HETSS element to the grouping mentioned above creates some non-uniformity of heat flux density distribution which was found not to have exceeded 8%, as can be deduced from Fig 3.

4. Experiments

Since the present measurements form part of a code validation experiment as well as a flow optimization procedure aiming at establishing good cooling conditions for the SINQ liquid metal target window, he same flow geometry and flow rates used in local velocities measurements [1] were used in the test matrix for the HETSS measurements. So far two different geometric arrangements were examined, namely one in which the bottom end of the central guide tube was cut horizontally (referred to as "flat") and one where the tube was cut at an angle (referred to as "slanted"). In both cases the clearance between the guide tube and the hemispherical cap was varied. The "gap width" quoted is the distance between the bottom edge of the guide tube and the hypothetical line of its intersection with the cap (vertical distance). In the case of the slanted cut the average distance, i.e. the distance at half height of the slanted cut is quoted (cf. Fig. 5)

4.1 Guide tube with horizontal bottom edge

For a flat bottom edge of the central guide tube one intuitively expects a stagnant zone and hence a peak in the wall temperature at constant heat flux density near the center of the cap. The fluid is expected to heat up on its way to that zone and, therefore, an increase in wall temperature is expected from both ends of the HETSS ribbon. The latter is actually observed, in particular for small gap widths, as can be seen from Fig. 6, which gives the 50 second time average of the temperature rise in the wall per unit heat flux for different flow configurations (gap widths and flow rates in the loop as defined above). Contrary to intuition, there is no peak in the center of the ribbon. This may be attributed to the combination of two effects: (1) since the ribbon has constant width while the flow channel effectively narrows as the fluid moves down the cap, cold fluid flows over the HETSS from the side and contributes to a lower wall temperature in the measuring geometry than would be obtained in a real axisymmetric configuration and (2) there is not real stagnation of flow at the apex of the cap, at least not when averaged over the area of one HETSS unit and over reasonable amounts of time. While the first effect is an artifact of the present HETSS geometry, the second one may be important in a real situation.

Since the heaters in the HETSS are extremely thin they have practically no thermal inertia. The temporal stability of flow can, therefore, be estimated by using different averaging times. The signals were integrated over nine different time periods between 0.1 and 50 seconds. As can be seen from Fig. 7, where the third dimension in the plots is averaging time, the difference between long and short averaging is more pronounced for high flow rates and large gaps. The instantaneous temperature can exceed the averaged value significantly. In our observations we found up to a factor of two, even though our spatial average is 4 cm^2. In a real situation with a thick wall the fluctuations would probably be significantly smaller due to thermal inertia.

The assumption that cooling in the cap is considerably more efficient than in a stagnant situation is also corroborated by the observed level of temperature increase, which is of the order of 3K or less in all cases. According to calculations, the heat flux density of

$7W/cm^2$ would create about 80K of temperature drop in a stagnant layer of 1 cm of mercury. This was also verified experimentally: In the configuration shown in Fig. 8 the bottom temperature of a 1 cm thick horizontal mercury layer was stabilized by flowing water, while the top surface was heated with 7 W/cm^2. The single HETSS element which was used to generate the power reached a temperature of 76K above the bottom temperature.

The experiments thus confirm that, instead of an axis-symmetrical, two-dimensional flow structure there exists a more complicated one which is more beneficial for cooling the wall. The differences in temperature distribution along the HETSS at short and long averaging times suggest the presence of large scale turbulent perturbations. The expansion of flow cross section after the gap is, of course, a very powerful turbulization mechanism. If the bottom end of the guide tube is below the center of the hemispherical cap, the possibly slightly turbulent flow coming down the ring space between the two tubes passes though a zone of narrowing cross section, which is an effective laminarization mechanism. The thermal boundary layer accumulates heat in this local laminar area and is attacked by turbulence when the laminar jet loses its power. This laminar jet is less pronounced at large gap width, and hence the measured wall temperature is more dominated by the turbulent flow and is, therefore, lower. Also the absence of a central peak at small gap widths is attributed to the effect of turbularization at the edge of the guide tube

Since this turbulent fluctuations prevail on a short time scale and the velocity vector at any position can change sign, the averaged velocity field for such an unsteady flow structure can well show a stagnant area in the central part of the cap. Another possible mechanism which can result in the same cooling effect might be connected with azimuthal velocities in the system. The two configurations are sketched in Fig. 9. Effective cooling of the bottom area could be caused by the vertical vortex which usually arises in center-directed velocity flows (in the bath tub, for example). It is observed in MHD experiments that the axes of such vortices change their positions chaotically. Again, the HETSS strip will be very sensitive to such cooling.

4.2 Guide tube with slanting bottom edge

The purpose of cutting the bottom edge of the inner guide tube at an angle was to destroy the axial symmetry and by this token move any flow stagnation zone away from the apex of the hemispherical cap, where heating would be most intense in the real situation in SINQ.

Examples of our results shown in Fig. 10, which were taken with the HETSS arranged in the plane of the slanted cut (cf. Fig. 5), do not indicate any drastic non-symmetry in the temperature distribution. The narrow gap was at the side of the HETSS units with the low index numbers. Although the two peak structure is not as pronounced as in the case of the flat bottom edge guide tube, no indication of any flow structure improvement by sloping the guide tube end is obvious from these experiments. If any, the temperatures in the cap center seem to be even slightly higher, especially at high flow velocities. The reason

might be the destruction of some favorable flow structure by the asymmetry, because significant azimuthal velocity structures will not be able to develop in this geometry.

4.3 Importance of thermal convection

An alternative explanation to the one given above for the existence of the two peak structure involves the role of thermal convection, assuming that a stagnation zone in the forced flow exists at all times near the bottom of the hemispherical cap. In order to estimate its importance, measurements were carried out at three different heat flux densities, namely 7, 3 and 1 W/cm^2. If thermal convection contributes to the heat removal to any significant extent, varying the heat flux density should destroy the proportionality between temperature and heat flux density. If the wall temperature per unit heat flux is the same at different heat flux densities, thermal convection plays no role even for the highest heat flux. The data reproduced in Fig. 11 show that the normalized temperature distribution is indeed independent of the heat flux density used for the 2 cm gap case and at flow rates of 1.2 l/s and more, where the temperature peaks are most prominent. This shows that the characteristic temperature maxima cannot be explained by thermal convection. It is, however, observable at low flow rates and at large gap widths where the normalized temperature can be seen to decrease with increasing heat flux.

5. Conclusions

The measurements reported here are the first extensive application of the newly developed HETSS technique. The results clearly show that the technique, although so far limited to rather low heat flux, is useful in measuring heat transfer coefficients.

The fairly effective cooling of the cap observed even for the flat bottom edge of the flow guide tube can be explained either by chaotic turbulence or by the development of a vortex that changes its orientation chaotically around the tube axis. Special vorticity measurement techniques could be developed to get better information about the instantaneous flow structure. For this purpose electric potential sensing in locally created magnetic field appears to be suitable.

The peak heat flux density at the SINQ beam window is expected to be about 10 times higher (70 W/cm^2) than the highest value generated by the HETSS. Since the measured normalized temperature jump is in the range of 1.5 - 2 K/(W/cm^2), this would mean that, if scaling is valid, the inner window surface would take on a temperature which is about 100 to 140 K higher than the temperature of the forward flowing liquid metal (ca 180°C). While this would not put the window temperature in a regime that is in any way dangerous for steel, it might be good to have more control over the situation than just rely on chaotic fluctuations. Therefore, a controllable jet will be directed across the beam window area by a special bypass pump in the next stage.

For this investigation we are considering a layout of the HETSS better matched to the real geometric situation and allowing to imitate the real distribution of heat flux in the SINQ beam window. In order to be able to use the existing equipment, the new arrangement is designed such that its units have the same area and the same electrical data as the present ones.

6. References

Y. Takeda, H. Kikura and G.S. Bauer "Measurements of Flow Configurations in a Mockup Target for SINQ", this conference

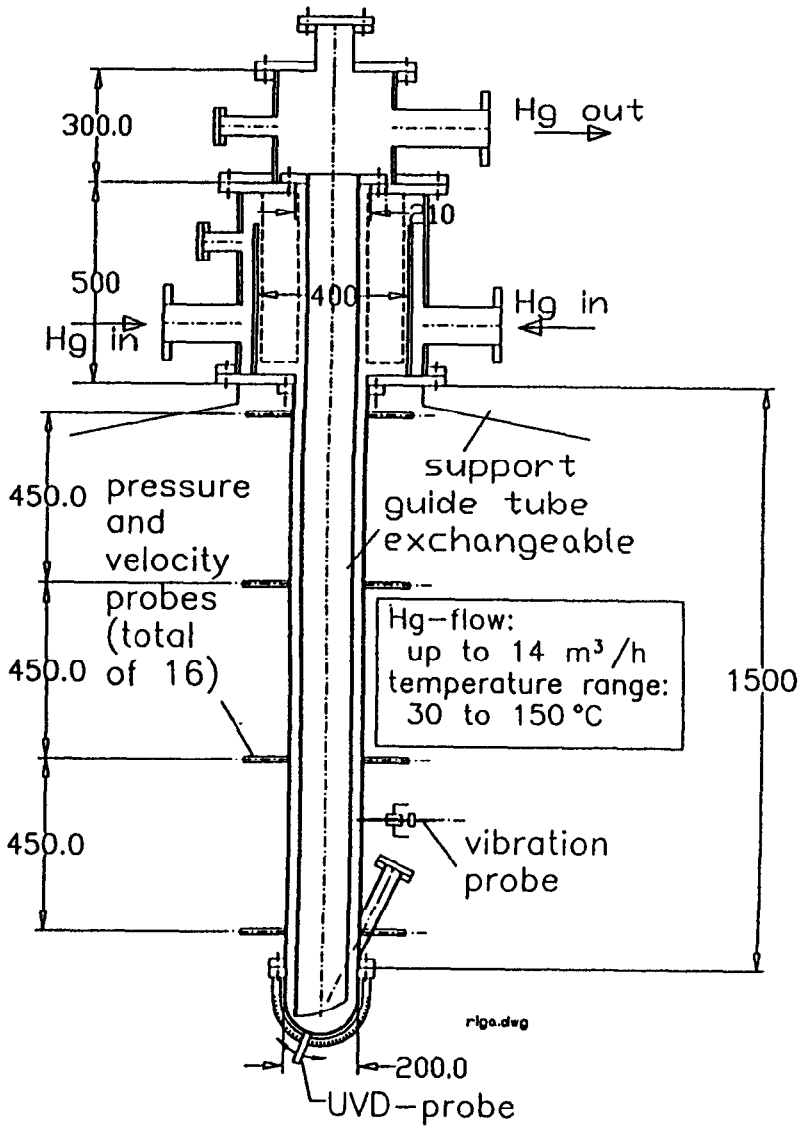

Figure 1: Schematic of the full scale SINQ target mock up installed at the mercury loop of the University of Latvia in Riga. The top half is only simulated with reduced height for flow rectification. The bottom cap and lower part of the guide tube can be exchanged.

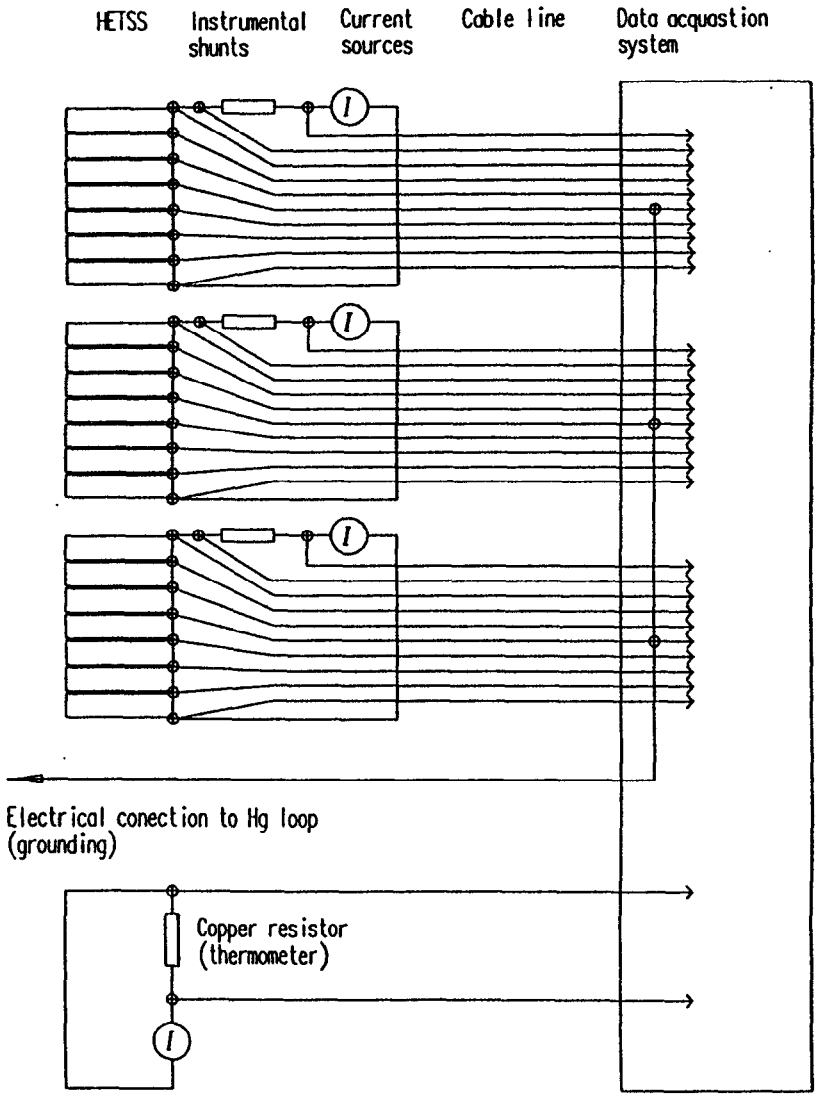

Figure 2: Power supply and voltage measuring scheme of three group of seven HETSS each used in the present experiment.

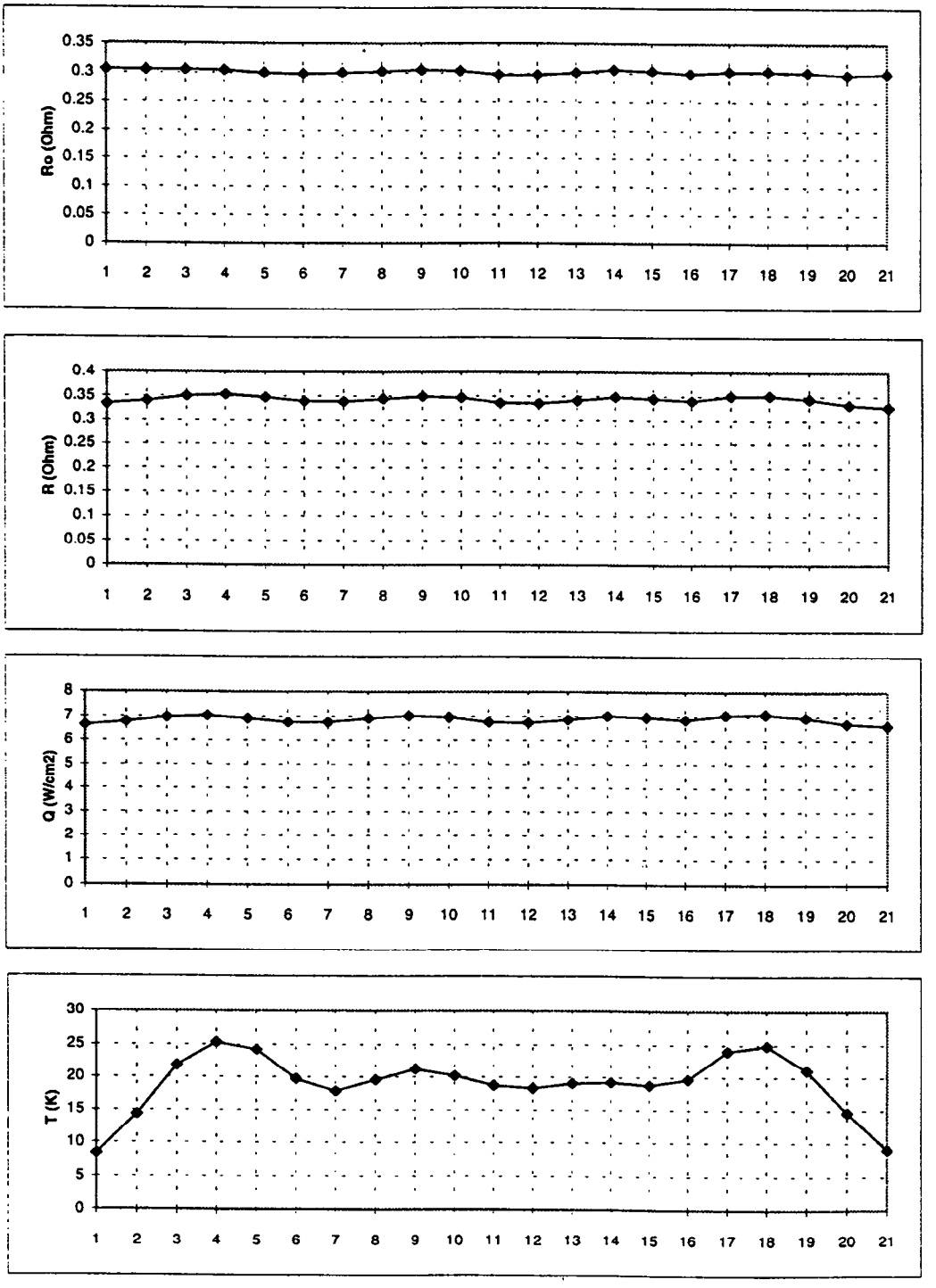

Figure 3: Top to bottom: resistance measured for the 21 HETSS with virtually no heat generation; - resistance measured at the heat flux distribution shown in the frame below; -- - measured heat flux distribution; - temperature above the inflowing fluid deduced for the 21 HETSS from the measured change in resistivity. Gap width was 2cm and flow rate was 0.6 l/sec.

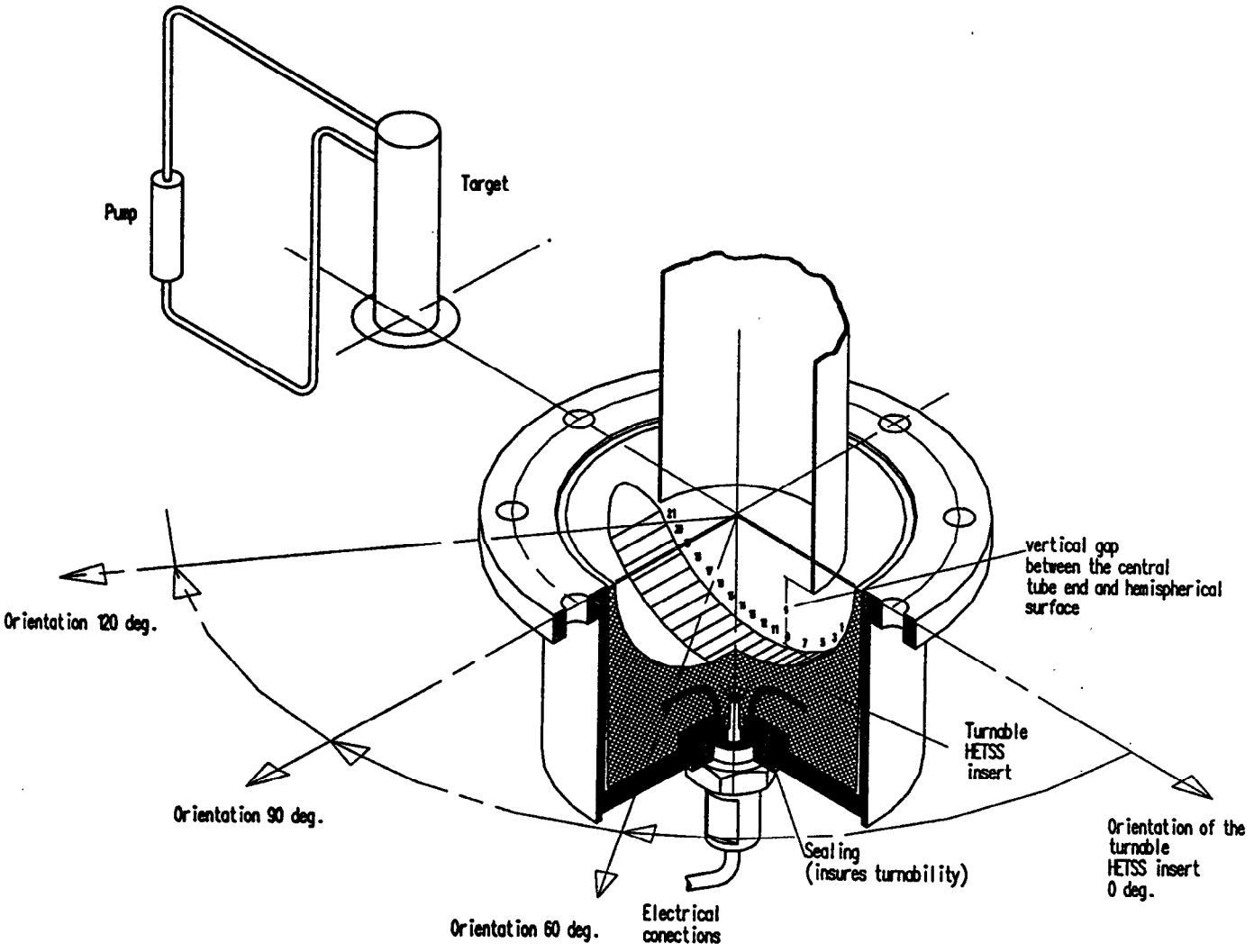

Figure 4: Sectional view of the HETSS-cap used for the heat transfer measurements and nomenclature for the orientation of the HETSS.

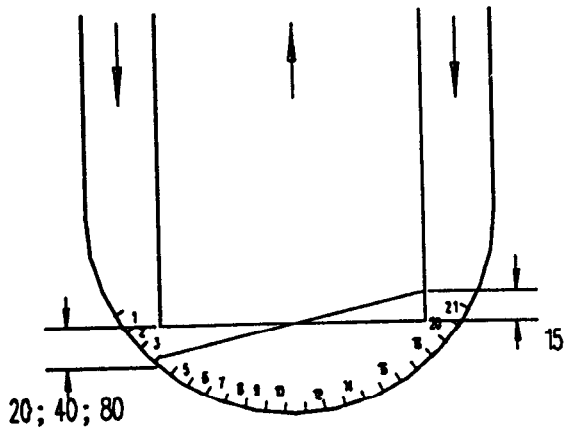

Figure 5: Schematic of the "flat" and "slanted" guide tubes and measure used for the "gap width" in the present experiments.

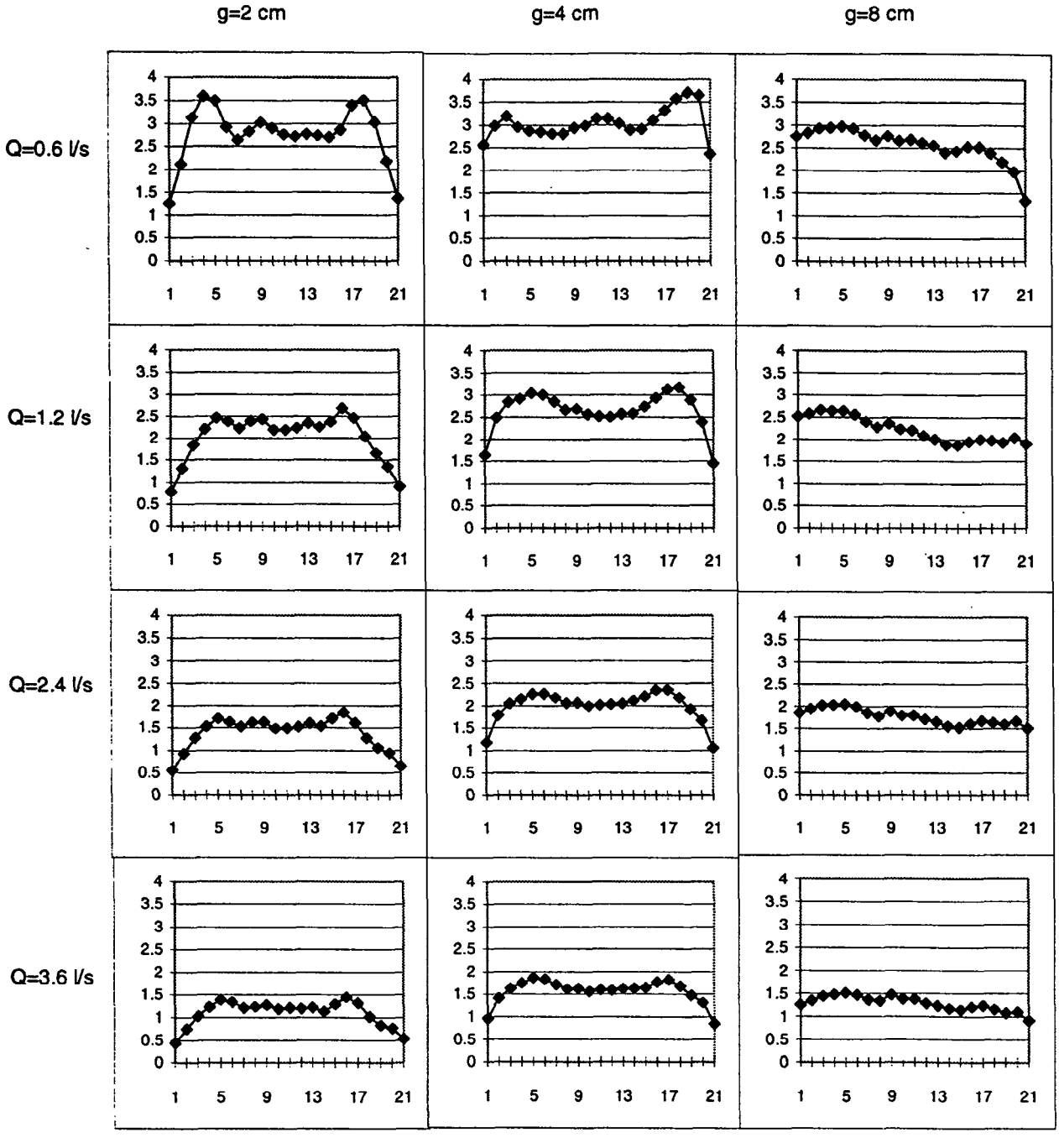

Figure 6: Local normalized temperature, in units of K/(W/cm^2), relative to the inflowing fluid as derived for the 21 HETSS elements at a heat flux density of 7 W/cm^2 for the 0° orientation according to Fig. 4 and for a flat bottom end of the guide tube. Q is the mercury flow rate and g is the gap width. Averaging in the measurement is over 50 seconds.

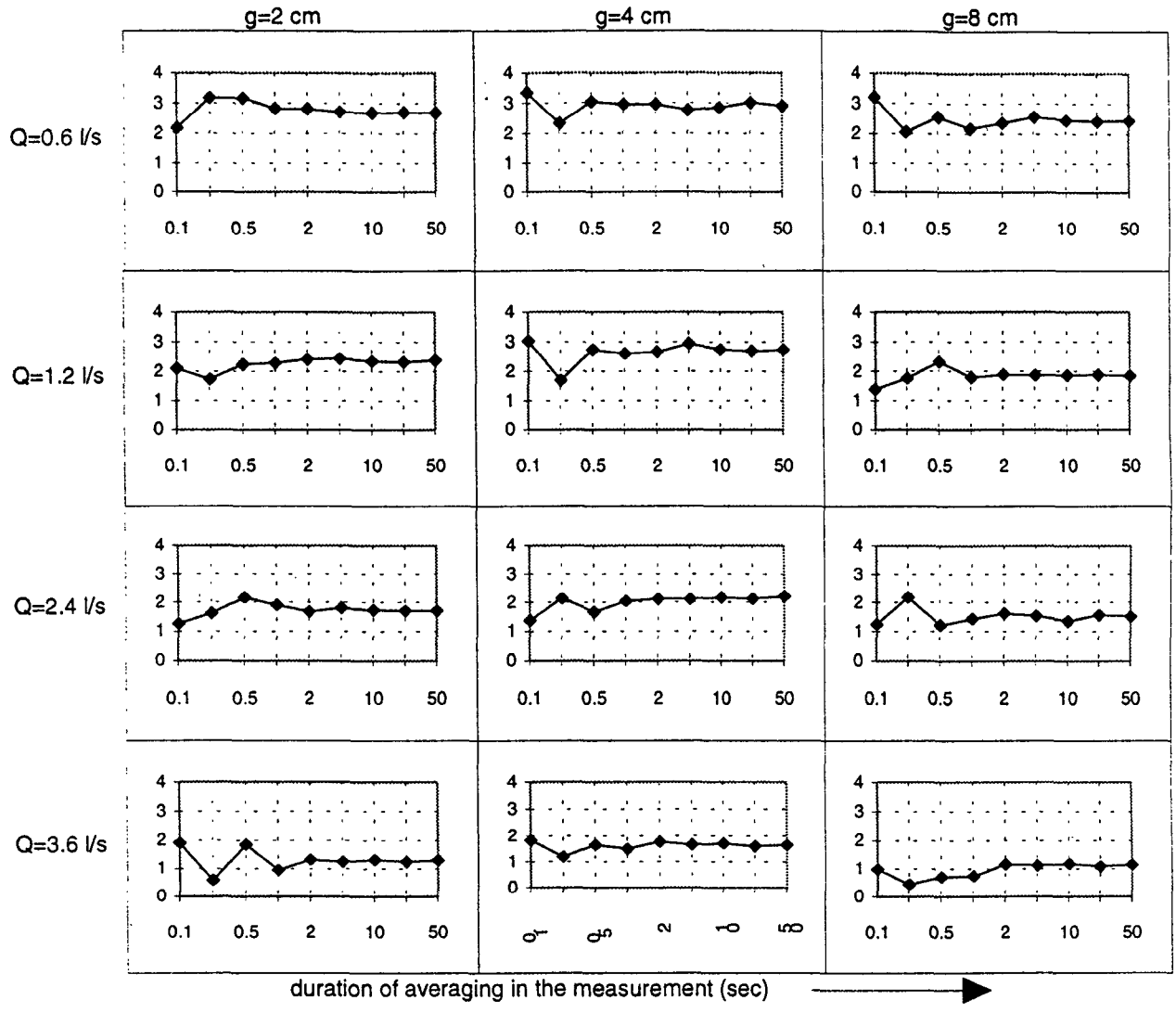

Figure 7: Local thermal temperatures deduced for the HETSS element Nr. 15 for different times of averaging. Measuring conditions are the same as in Fig. 6

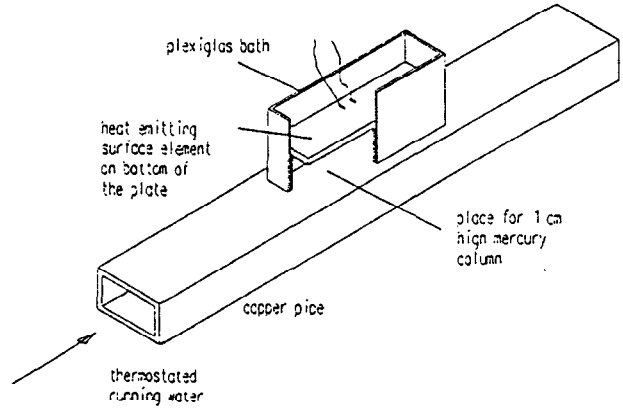

Figure 8: Arrangement used to determine the temperature rise of the HETSS for a stagnant layer of mercury.

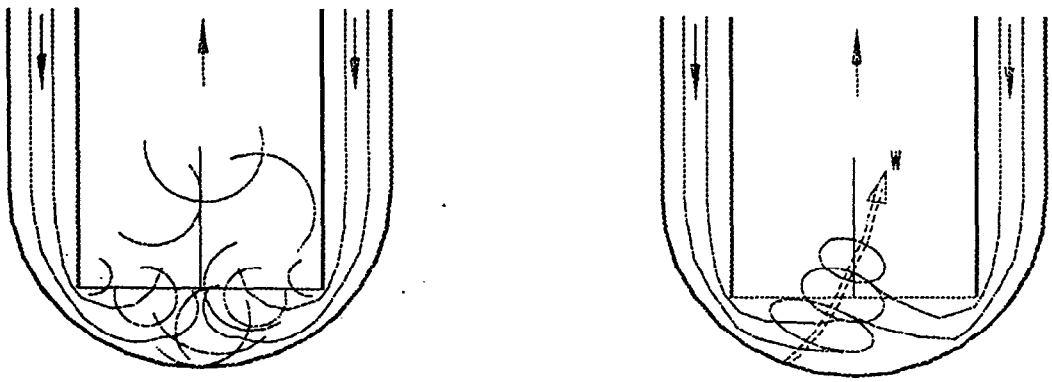

Figure 9: Schematic visualization of chaotic turbulence or vortex flow in the cap, both of which might be responsible for the observed good wall cooling.

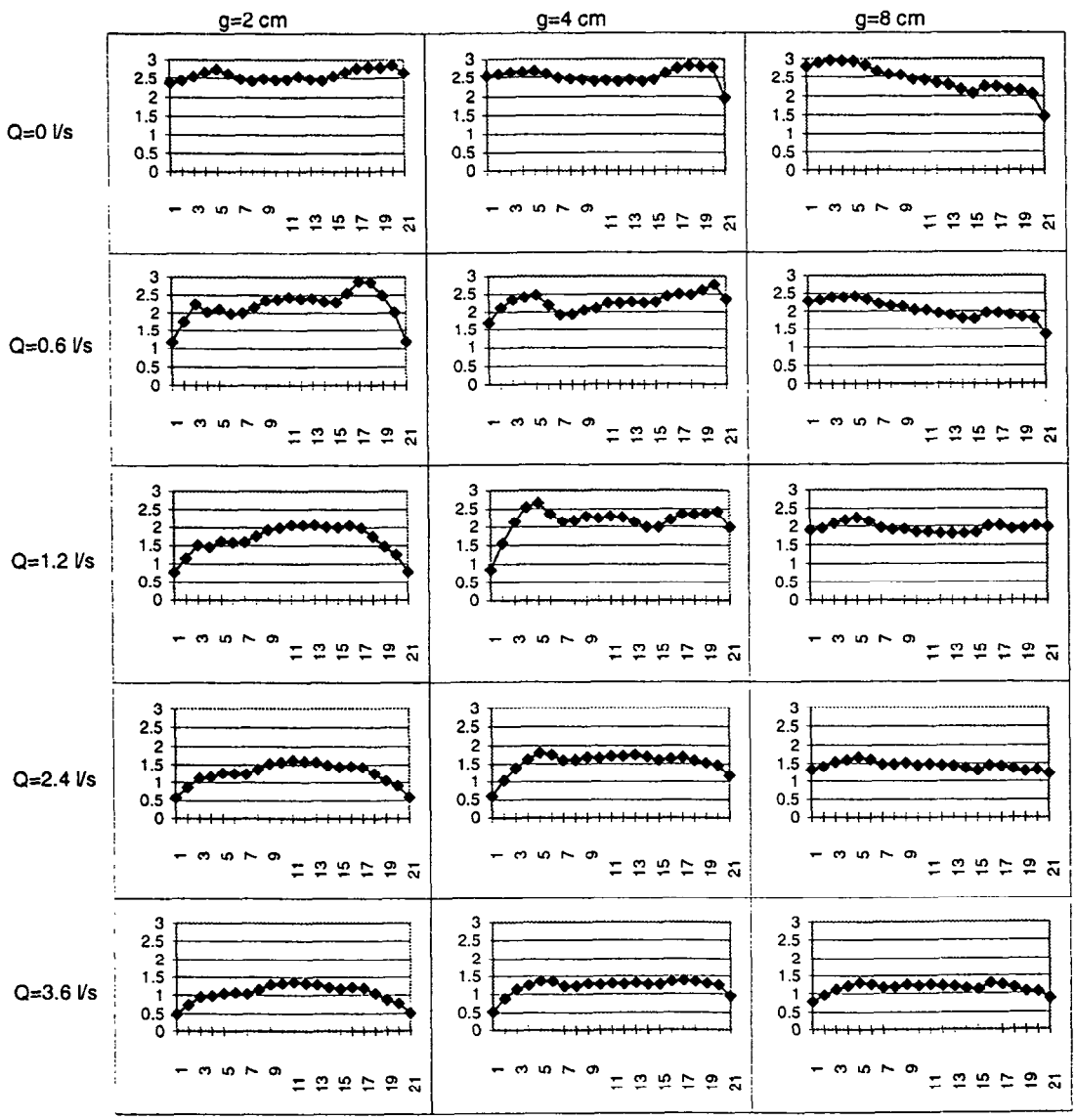

Figure 10: Local temperature distribution per unit heat flux density derived from measured resistance change in the 21 HETSS elements for a slanted cut of the guide tube as shown in Fig. 5a for different flow rates Q and nominal gap widths g.

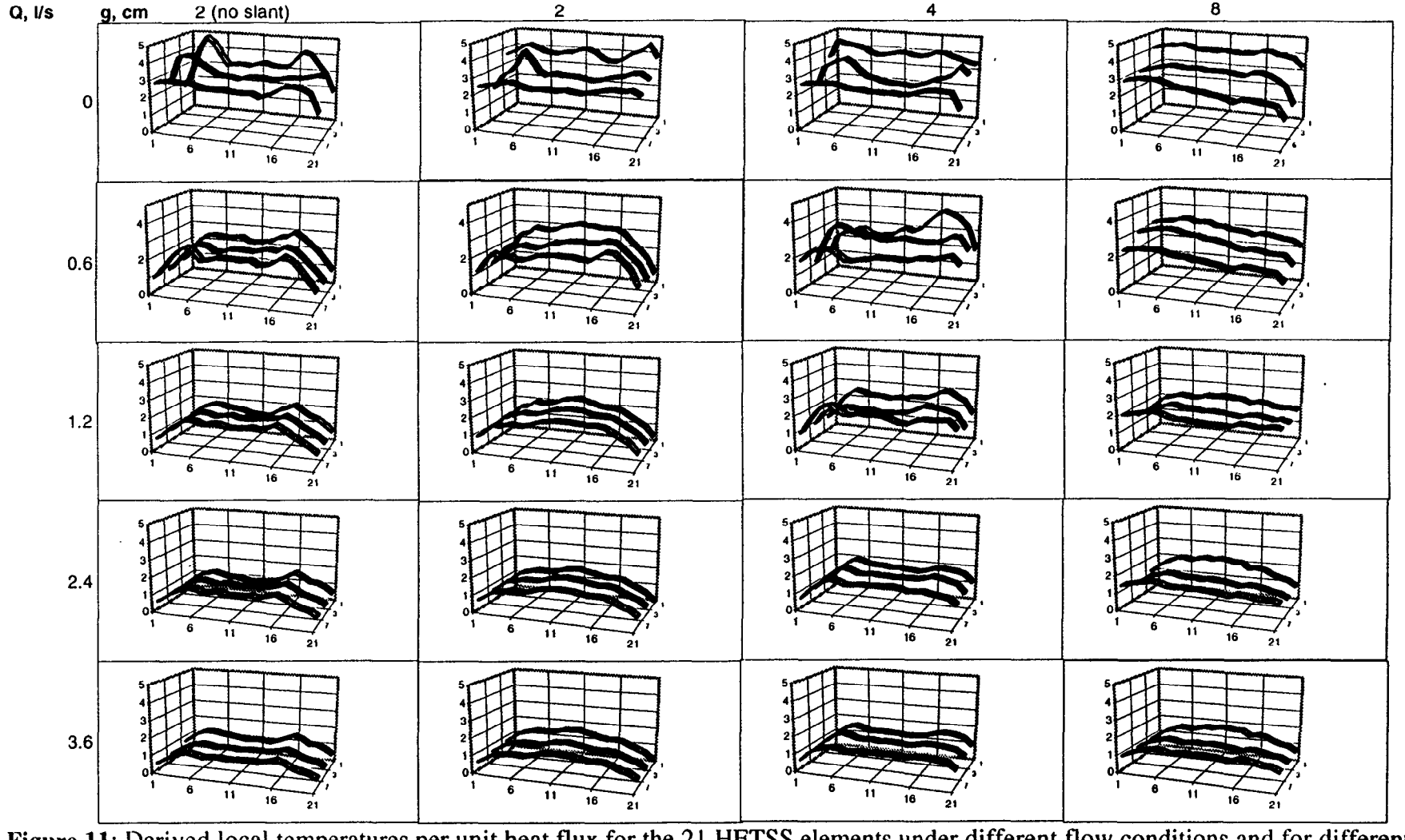

Figure 11: Derived local temperatures per unit heat flux for the 21 HETSS elements under different flow conditions and for different heat flux densities of 1, 3 and 7 W/cm^2 (parameter of the curves in each plot). At high flow rates above 1.2 l/s the temperatures are independent of heat flux density, showing that thermal convection plays no role. The first row of data is for the flat guide tube, the others are for a slanted bottom edge.